SAND--89-2656

SAND89-2656
Unlimited Release
Printed August 1990

DE91 000098

Attenuation Studies of Booster-Rocket Propellants and Their Simulants

Larry J. Weirick
Explosive Projects and Diagnostics Division
Sandia National Laboratories
Albuquerque, New Mexico 87185

Abstract

A series of impact experiments on a composite propellant, an energetic propellant, and their simulants was recently completed using a light-gas gun. Previous experiments[1] were done to obtain Hugoniot data, to investigate the pressure threshold at which a reaction occurs, and to measure spall damage at various impact velocities. The present studies measured the attenuation of shock waves in these materials, completing the shock characterization needed for material modeling. An initial impulse of 2.0 GPa magnitude and ~0.6 μs duration was imposed upon samples of various thicknesses. VISAR was used to measure the free-surface velocity at the back of the samples; these data were used to generate a curve of shock-wave attenuation versus sample thickness for each material. Results showed that all four materials attenuated the shock wave very similarly. Material thicknesses of 3.0, 7.62, 12.7, and 19.0 mm attenuated the shock wave ~16%, 33%, 50%, and 66%, respectively.

Acknowledgements

The author gratefully acknowledges the contributions of the following people, without whose assistance this program would not have been possible: John Matthews, 2514, who set up and operated the diagnostics and built the propellant targets; Mike Navarro, K-Tech Corp., who operated the gas gun; Heidi Anderson, K-Tech Corp., who built the projectiles and the simulant targets; Al McDonald, 8242, who initiated the program's need and provided program direction and liaison; Lloyd Bonzon, 2514, who gave managerial support, direction, and encouragement; Agnes Greb, K-Tech Corp., who was invaluable in instructing the author on transmission shots in general and attenuation shots in particular; and Bruce Kistler, 8242, who improved this paper considerably by his many explanations and discussions.

Contents

Introduction 7
Experimental Procedure 8
Composite Materials 8
Energetic Materials 9
Gas Gun 9
VISAR 9
Projectiles/Targets for Attenuation Setup 9
Results 10
Overall 10
H-19 12
TP-H1207C 13
UGS and the Energetic Propellant 14
Discussion 16
Summary 18
References 18

Figures

1 Illustration of hydrodynamic pulse attenuation 8
2 Schematic of projectile/target for attenuation shots 10
3 Plot of free-surface velocity with time for H-19 samples of various thicknesses 12
4 Attenuation profile for H-19 13
5 Plot of free-surface velocity with time for TP-H1207C samples of various thicknesses 13
6 Attenuation profile for TP-H1207C 14
7 Plot of free-surface velocity with time for UGS samples of various thicknesses 14
8 Plot of free-surface velocity with time for the energetic propellant samples of various thickness 15
9 Attenuation profile for UGS and the energetic propellant 16
10 Attenuation profiles for H-19, TP-H1207C, UGS, and the energetic propellant 16
11 Particle velocity at the front and rear of the H-19 target (SRI) 16
12 Attenuation profile for PBX-9404 from Setchell 18

Tables

1 Composite Formulations and Mechanical Properties 8
2 Energetic Formulations and Mechanical Properties 9
3 Attenuation Shot Results 11
4 K-Tech Corp. Transmission Data 17

Attenuation Studies of Booster-Rocket Propellants and Their Simulants

Introduction

This investigation was begun to aid in studies of the vulnerability and lethality of solid-propellant booster stages. The materials of interest are a composite propellant, an energetic propellant, and their simulants. Better characterization of the inert simulants will allow their use in testing wherever possible.

The shock Hugoniot of a material is determined by the relationship between the shock and particle velocities. This relationship can be determined experimentally from planar, gun-impact experiments and can for many materials be approximated by a linear fit:

$$U_s = C_o + SU_p \ , \qquad (1)$$

where U_s is the shock velocity, C_o is the initial bulk sound velocity, S is a constant, and U_p is the particle velocity.

The shock Hugoniots of the composite and energetic propellants, and their simulants, were reported in an earlier paper.[1] To summarize here, the values of initial density, ρ_o, initial bulk sound velocity, C_o, and S are 1.84 g/cm^3, 2.3 mm/μs, and 2.16, respectively, for TP-H1207C; 1.89 g/cm^3, 2.25 mm/μs, and 1.5, respectively, for H-19; and 1.85 g/cm^3, 2.2 mm/μs, and 2.66, respectively, for the energetic propellant and its simulant, UGS.

The detonability of composite propellants has been studied since their inception. A recent study was done at Lawrence Livermore National Laboratory[2] (LLNL) on the detonability of a composite propellant. Delayed explosions were observed in the impact-damaged propellant at impact pressures above 3.0 GPa. The pressure threshold for a reaction to initiate in the composite propellant TP-H1207C was found to be ~4.0 GPa.[1]

The sensitivity and power of energetic propellants were studied in the 1970s at LLNL.[3] This work, together with investigations by SRI International and others, was summarized in a report from the High-Energy Propellant Safety (HEPS) Committee.[4] More recently, a study was done at LLNL on the detonability of energetic propellants.[5] They found a delayed detonation threshold of 0.62 GPa and a shock detonation threshold of 1.32 GPa for the most energetic of these propellants. The pressure threshold for a reaction to proceed in the energetic propellant from a direct impact was found to be above 0.53 GPa, but below 0.91 GPa.[1] The detonation threshold was estimated to be ~2.0 GPa.[1]

The process of spallation has been studied in a number of laboratories with a view to obtaining the criteria for dynamic fracture at high stress rate. Tension is induced within a sample by allowing a stress wave to reflect as a rarefaction from a free surface. The tension increases by interaction of the rarefaction wave with the primary wave until a critical value is reached and fracture occurs. The fact that the free-surface velocity stops dropping and then rises ("spall rebound or pullback") is due to the generation of compressive waves at the spall plane that increase the pressure. The clearly defined onset of fracture at a specific value of pullback suggests a characteristic material strength that corresponds to a damage threshold tension. This material property is referred to as the incipient fracture strength or spall strength, σ. The value of σ may be approximately related to the observed pullback by considering the interaction of the reflected wave with the primary wave, assuming a perfect reflection at the free surfaces.[6] The resultant expression is:

$$\sigma = 1/2\, C_o \rho_o \Delta\mu \ , \qquad (2)$$

where C_o is the initial bulk sound velocity, ρ_o is the material density, and $\Delta\mu$ is the measured pullback. The incipient fracture is understood in material terms as the macroscopic yield stress necessary for the growth of internal voids into a free surface or spall plane. The spall strengths of TP-H1207C and H-19 were measured as 0.022 and 0.018 GPa, respectively, and of the energetic propellant and UGS as 0.033 and 0.022 GPa, respectively.[1]

It is generally well known that a square pulse, introduced at the surface of a material that will not

support a shear wave, evolves to a triangular pulse as it propagates through the material (Figure 1). The speed of propagation of the front is associated with the slope of the Rayleigh line and, in the absence of viscosity, this front propagates as a shock. The rarefraction wave, on the other hand, is governed by a reversible adiabatic process where the sound speed immediately behind the shock front is greater than the shock velocity and decreases with decreasing pressure. The result is that the peak pressure and the slope of the expansion wave both decrease with propagation distance, and the length of the pulse increases. This phenomenon, called hydrodynamic attenuation, is exhibited by most materials.

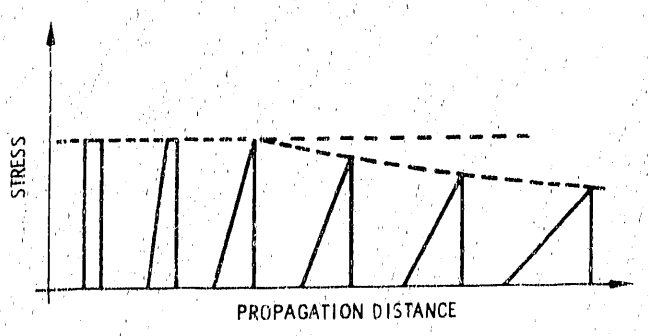

Figure 1. Illustration of hydrodynamic pulse attenuation

The objective of the present study is to obtain attenuation data for the two propellants and their simulants. This information is needed in order for a complete materials model to be used in a code called WONDY.[7] WONDY can then be used to predict the extent of propellant spallation on the inside of a propellant core in a rocket booster that has been shocked by a laser beam.

Experimental Procedure

Composite Materials

One propellant, TP-H1207C, and its simulant, H-19, are of composite formulation, and the other propellant, the energetic and its simulant, UGS, are based upon energetic formulations, as given in Tables 1 and 2.[8] None of the materials have any significant porosity. The H-19 contains large, rectangular crystals of potassium chloride and small, spherically shaped particles of metallic aluminum. The matrix that binds these constituents together is an hydroxy-terminated, polybutadiene-polyurethane polymer (HTPB). The TP-H1207C propellant formulation is based upon ammonium perchlorate with aluminum additions and bound together with the HTPB. The "static" mechanical properties of these materials are given in Table 1. The tensile strengths are relatively low (~0.001 GPa) and the elongations are moderate (~50%). Densities of ~1.8 g/cm^3 are typical of solid propellants.

Table 1. Composite Formulations and Mechanical Properties

		TP-H1207C	H-19 (wt. %)
Composition:			
Fuel	Aluminum	Al	31.75
Oxidizer	Ammonium perchlorate	AP	5.0
Inerts		KCl	51.5
Polymers	Hydroxy-terminated polybutadiene	HTPB	8.8
Curatives		IPDI	0.7
Plasticizer		DOA	2.0
Bonding agent		Tepanol	0.2
Processing aid		ODI	0.04
Cure catalyst		TPB	0.02
Mechanical Properties:			
Density (g/cm^3)		1.84	1.89
Tensile strength (psi/GPa)		140.0/0.001	114.0/0.008
Maximum elongation (%)		45.3	32.0
Tensile modulus (psi)		637.0	450.0

Table 2. Energetic Formulations and Mechanical Properties

	Energetic	UGS (wt. %)	
Composition:			
Fuel	Double-base propellant	DBP	19.7
	Aluminum	Al	5.0
Oxidizer	HMX	HMX	0.0
	Ammonium perchlorate	AP	0.0
Inerts		$NaSO_4$	65.3
Polymers		HDAP	9.0
Curatives		N100	1.0
Processing aid		HDI	0.04
Mechanical Properties:			
Density (g/cm^3)	1.85		1.85
Tensile strength (psi/GPa)	100.0/0.0007		158.0/0.011
Maximum elongation (%)	250.0		50.0
Tensile modulus (psi)	450.0		490.0

Energetic Materials

The energetic propellant formulation is based upon a double-base mix of nitrocellulose and nitroglycerin. It also contains aluminum and HMX. The UGS simulant contains large, rectangular crystals of sodium sulphate and small, spherically shaped particles of aluminum. The matrix that binds these constituents together is a mix of hexane, diol, adipate, and phythalate (HDAP) and the double-base propellant. The "static" mechanical properties of these materials are given in Table 2. The tensile strength of these materials is very low (near 0.001 GPa). The elongation value for the simulant UGS is moderate at 50% and the value for the energetic propellant is relatively high at 250%. Densities near 1.85 g/cm^3 are typical of solid rocket booster propellants.

Gas Gun

The light-gas gun system used has previously been described in detail.[9] Briefly, the barrel is 9 m long, with an inside diameter of 63.4 mm. The breech is of a quick-acting, quick-change design with two inserts. One is termed a "wraparound" for low-velocity shots using nitrogen (below 0.5 km/s). A second is called a "dual-diaphragm" for higher-velocity shots using helium (up to 1.5 km/s for projectiles with weights below 0.2 kg).

VISAR

One modern technique used for measurement of shock phenomena is the VISAR (Velocity Interferometer System for Any Reflector).[10] A "Push-Pull" VISAR method developed by Hemsing[11] and used in these experiments results in effective cancellation of self-light from a reaction. An important variation on the Push-Pull VISAR is a system that has an extended (166 cm long) air-delay leg in place of the quartz-delay leg. This replacement allows the accurate measurement of particle velocity in a very low velocity regime (below 0.1 km/s).

Projectiles/Targets for Attenuation Setup

Figure 2 is a schematic of the projectile and target configurations for these attenuation experiments. A 5-cm-diameter sample of propellant/simulant was epoxied to an aluminum ring holder on the target mount. Sample thicknesses were 2.54, 5.08, 7.62, 10.16, 12.7, and 19.05 mm. A 0.01-mm-thick piece of aluminum foil was epoxied with urethane cement to the back side of the propellant/simulant disk to function as a reflecting mirror for the laser beam. This mirror was considered a "free surface." The projectiles were made from aluminum and had a 1-mm-thick PMMA disk (low-impedance impactor) attached to a 6.35-mm-long aluminum standoff ring at the front of the projectile. A 6.35-mm-thick piece of low-density carbon foam was epoxied between the PMMA and aluminum projectile to function as a mechanical support for the thin PMMA disk as well as a spacer from the aluminum projectile.

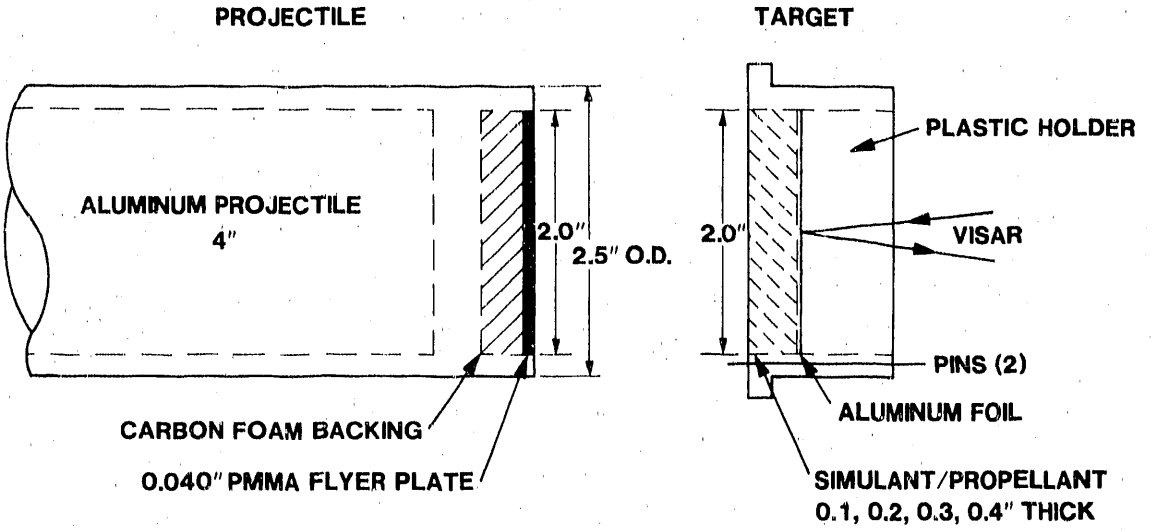

Figure 2. Schematic of projectile/target for attenuation shots

Results

Overall

A summary of the initial material conditions and final results for the attenuation experiments is given in Table 3. The information in the table includes the shot number; the measured thickness of the PMMA flyer plate; the measured thickness of the propellant/simulant target; the measured thickness of the carbon foam backing material; the measured velocity of the aluminum projectile; the measured and, if different, the calculated transit time for the passage of the shock wave through the sample; and the measured free-surface velocity and corresponding pressure calculated from Hugoniot data.

Table 3. Attenuation Shot Results

Shot No.	Flyer Thickness (mm)	Target Thickness (mm)	Target Backing	Projection Velocity (mm/μs)	Transit Time (μs)	Free-Surface Velocity (mm/μs)	Rear-Surface Pressure (GPa)
H-19:							
226	1.168*	07.62	None	0.871	2.71	0.57	NA
227	1.092	10.16	None	0.840	3.59	0.46	1.12
228	1.067	05.08	CF†	0.850	1.80	0.62	1.59
229	1.016	02.54	CF	0.850	0.90	0.70	1.83
240	1.016	07.62	None	0.857	2.71	0.51	1.26
UGS:							
230	1.016	07.11	CF	0.846	2.53/2.29	0.50	1.32
231	1.016	12.45	CF	0.854	4.49/3.96	0.39	0.98
TP-H1207C:							
233	1.016	12.70	None	0.852	4.21	0.45	1.16
234	1.016	07.62	None	0.850	2.45	0.56	1.49
235	1.016	10.16	None	0.854	3.28	0.47‡	NA
236	1.016	05.08	None	0.856	1.65	0.65	1.79
237	1.016	02.54	None	0.843	0.83	0.70	1.98
239	1.016	19.05	None	0.858	6.20	0.32	0.77
Energetic:							
238	1.016	12.70	None	0.840	4.47/4.03	0.39	0.98
241	1.016	07.62	None	0.867	2.90/2.42	0.61‡	1.60

*Flyer thickness greater than normal
†CF – 6.35 mm carbon foam, $\rho_0 = 0.2$ g/cm^3
‡Bad data point

H-19

Figure 3 shows the results from the attenuation experiments on four H-19 samples with nominal thicknesses of 2.54, 5.08, 7.62, and 10.16 mm (0.1, 0.2, 0.3, and 0.4 in.), respectively. Zero time is set at impact. The free-surface velocity was measured at the back of the samples using the VISAR system. The transit times measured for the passage of the shock wave through these H-19 samples agree with values calculated from Hugoniot data for the corresponding sample thicknesses. Although the velocity profiles seem to indicate that there was no unloading of the samples after passage of the shock wave, the correct interpretation is that the back of the sample spalled and the VISAR measured the spall pieces flying away at velocities initially equivalent to twice the particle velocity.

Using the Hugoniot data previously obtained for H-19[1] and the maximum free-surface velocities shown in Figure 3, the corresponding rear-surface pressure for a given sample thickness can be determined. These data are shown in Figure 4 and make up the attenuation profile for H-19. The nominal value for the initial impact pressure for each of the samples is also shown in the figure.

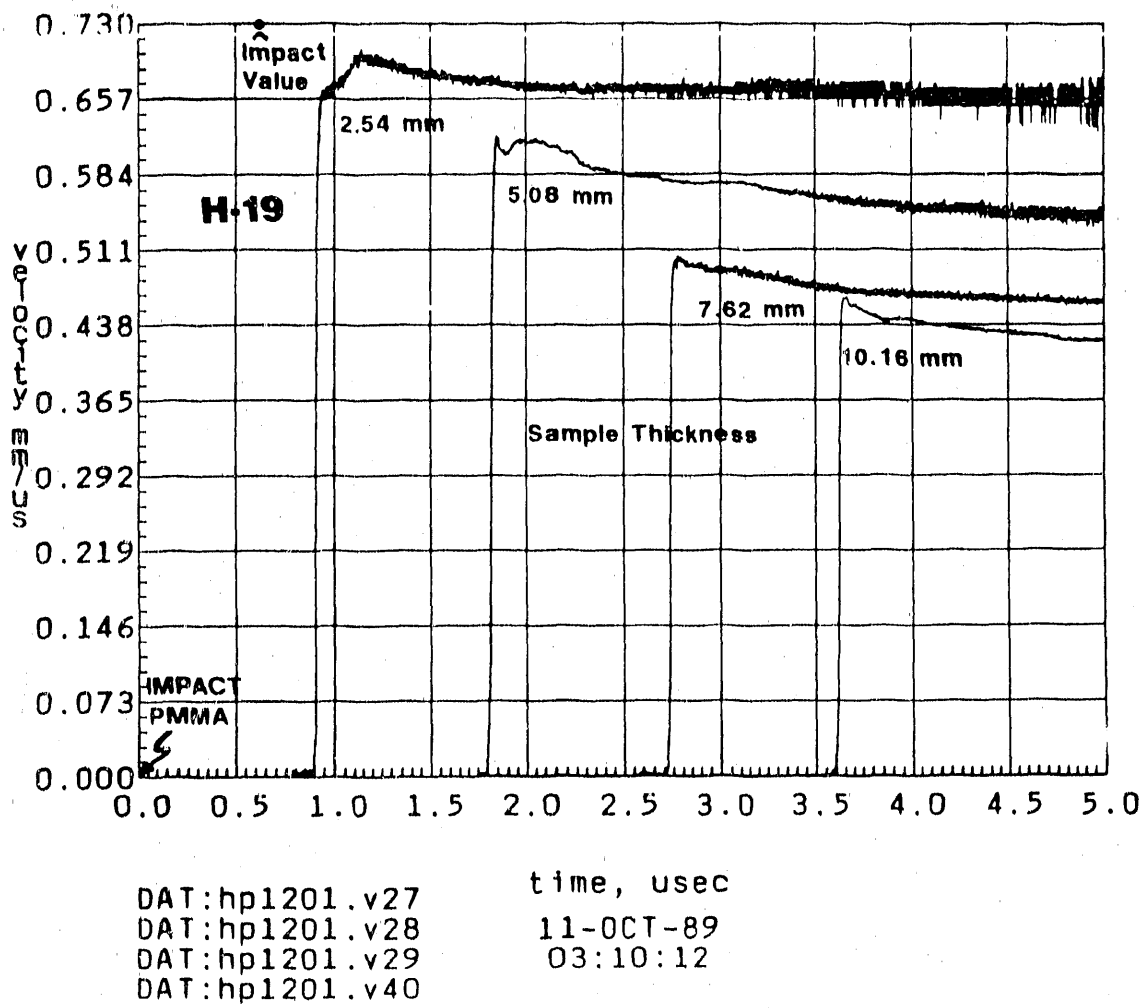

Figure 3. Plot of free-surface velocity with time for H-19 samples of various thicknesses

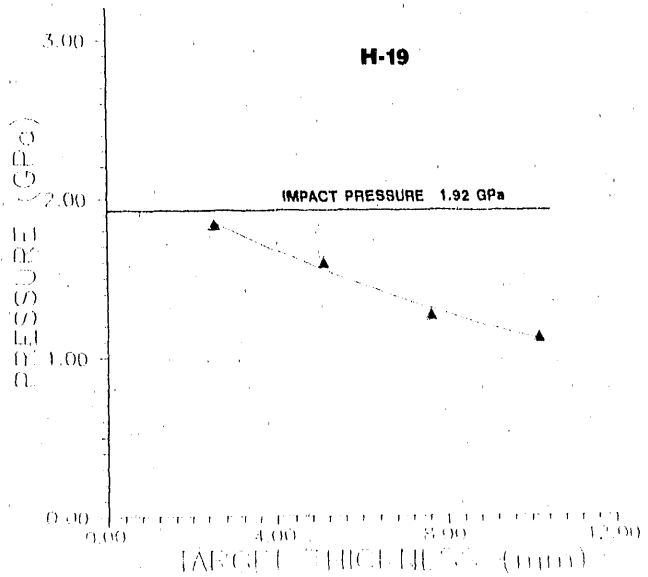

Figure 4. Attenuation profile for H-19

TP-H1207C

The results from the attenuation experiments on five TP-H1207C samples are shown in Figure 5. The TP-H1207C samples had nominal thicknesses of 2.54, 5.08, 7.62, 12.70, and 19.05 mm (0.1, 0.2, 0.3, 0.5, and 0.75 in.), respectively. Zero time is set at impact. The transit times measured for passage of the shock wave through these TP-H1207C samples agree with values calculated from Hugoniot data for the corresponding sample thicknesses. Again, the velocity profile reflects the movement of the back of the sample away from the primary piece after spallation. The maximum value of the free-surface velocity is twice the equilibrium particle velocity. Using these values of particle velocity and Hugoniot data,[1] the equilibrium rear-surface pressure can be calculated. The attenuation profile for TP-H1207C is shown in Figure 6.

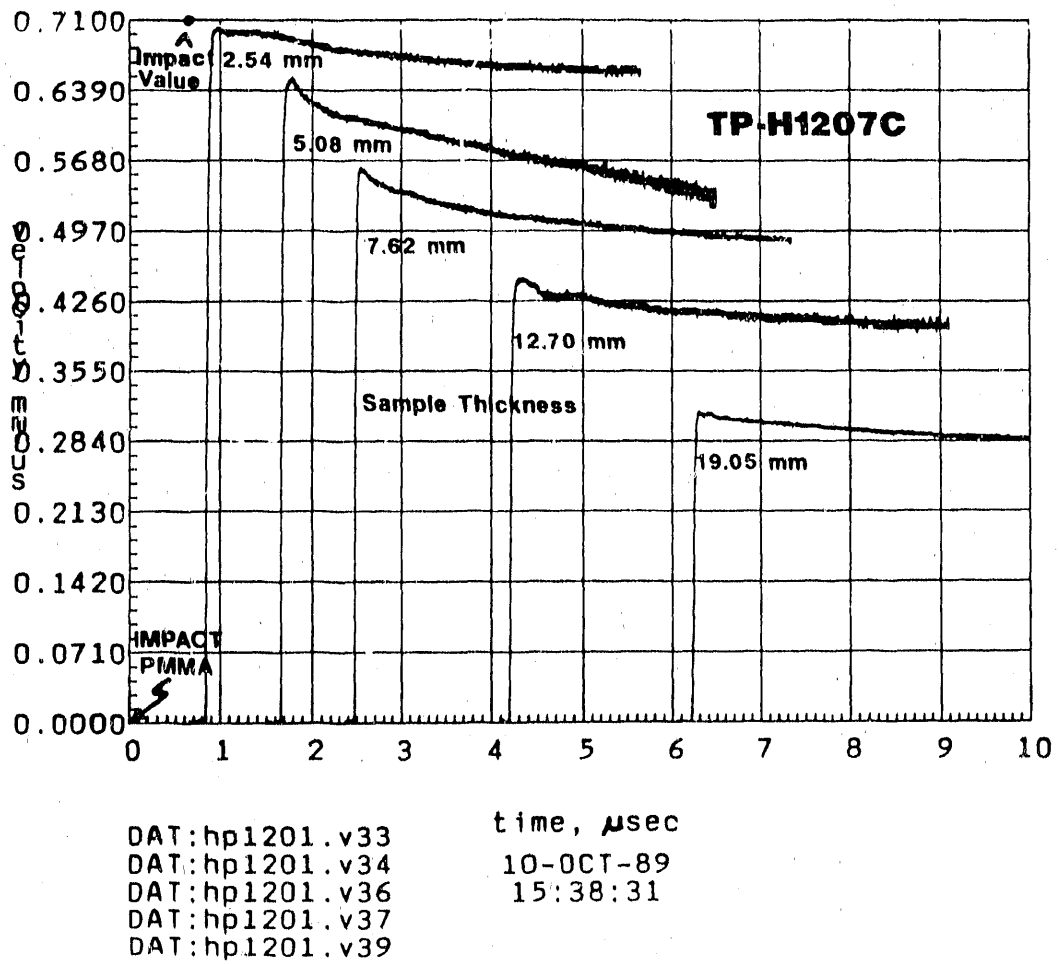

Figure 5. Plot of free-surface velocity with time for TP-H1207C samples of various thicknesses

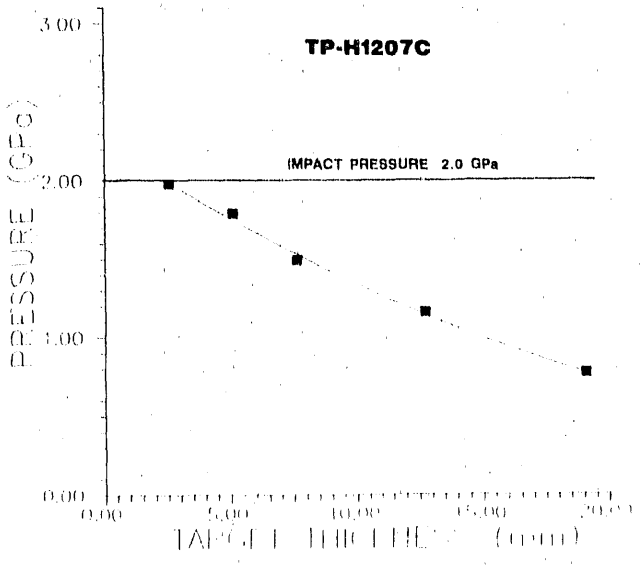

Figure 6. Attenuation profile for TP-H1207C

UGS and the Energetic Propellant

Figures 7 and 8 show the results for the attenuation experiments on two UGS and two energetic propellant samples, respectively. The samples had nominal thicknesses of 7.62 and 12.70 mm, respectively. The recorded transit times for the passage of the shock wave through these materials were significantly longer than those calculated from the Hugoniot data, as shown in Table 3. Using the Hugoniot data measured previously[1] and the maximum particle velocity obtained from the data shown in Figures 7 and 8 results in the attenuation profile of rear-surface pressure versus material thickness as shown in Figure 9 for both UGS and the energetic propellant.

The pressure-versus-thickness profiles for all four materials are plotted in Figure 10. The similarity in attenuation for all four materials can be easily seen from these plots.

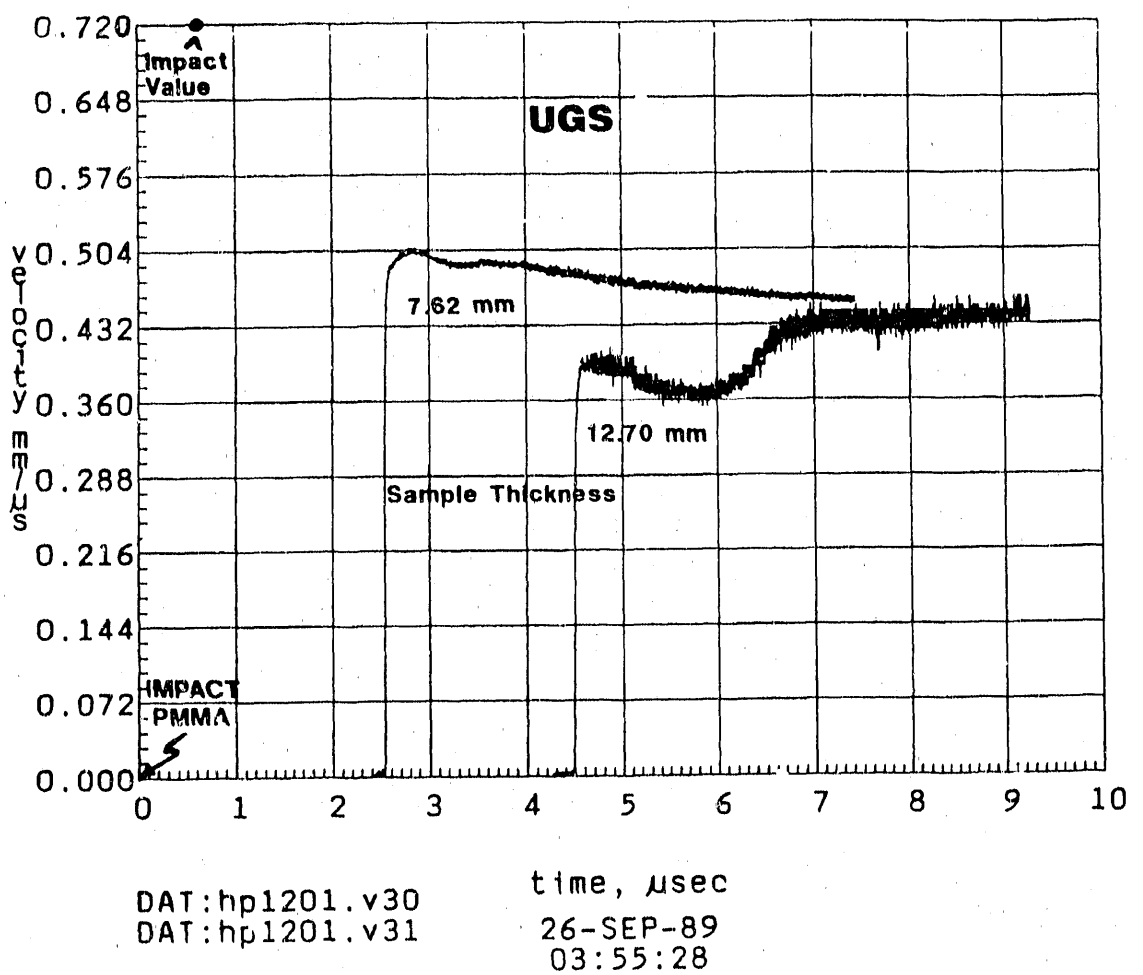

Figure 7. Plot of free-surface velocity with time for UGS samples of various thicknesses

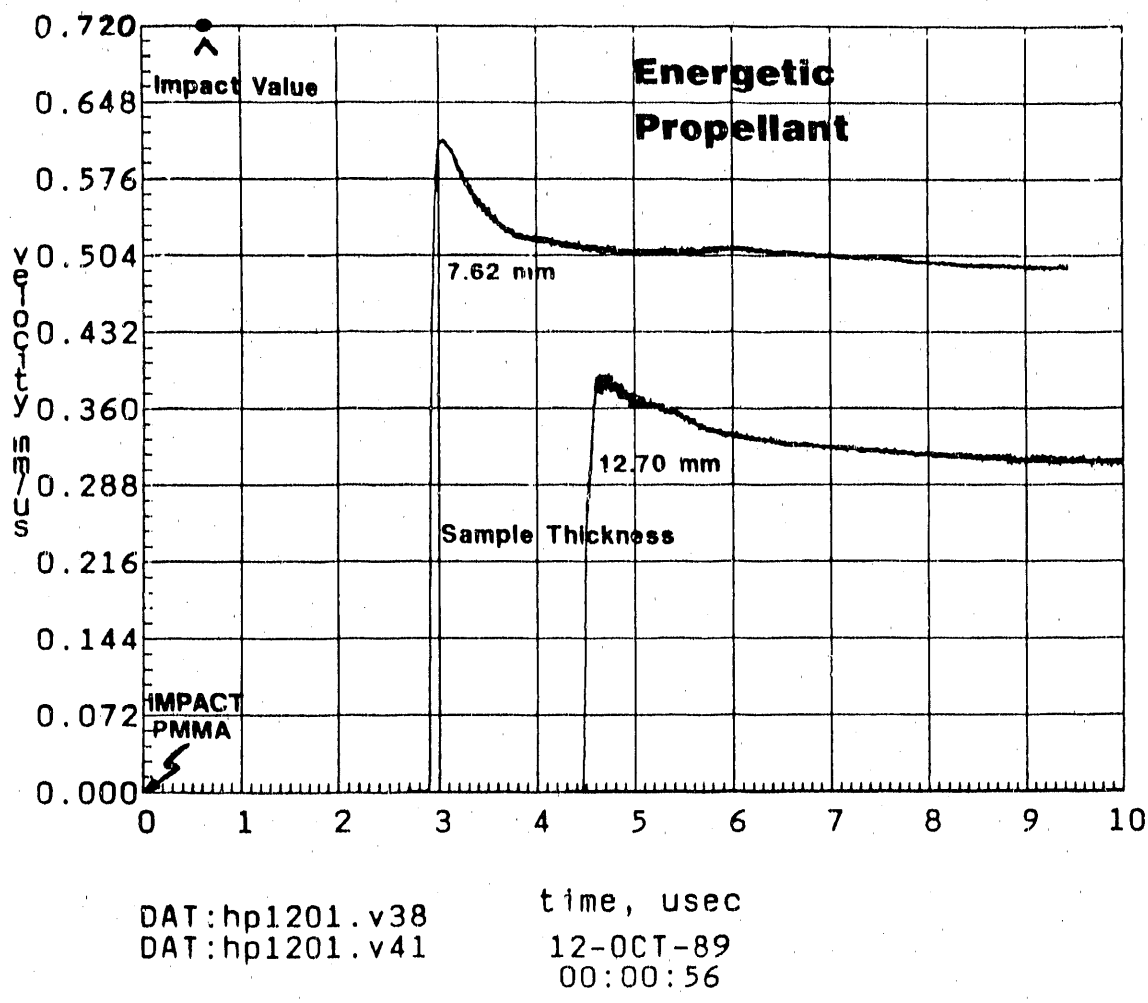

Figure 8. Plot of free-surface velocity with time for the energetic propellant samples of various thickness

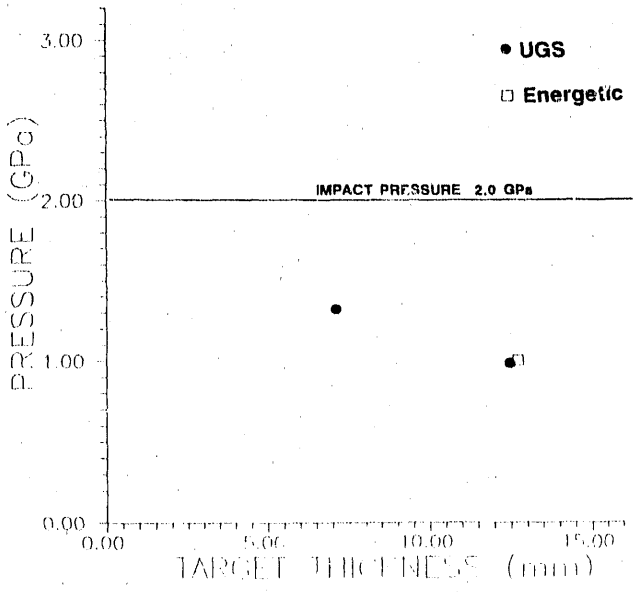

Figure 9. Attenuation profile for UGS and the energetic propellant

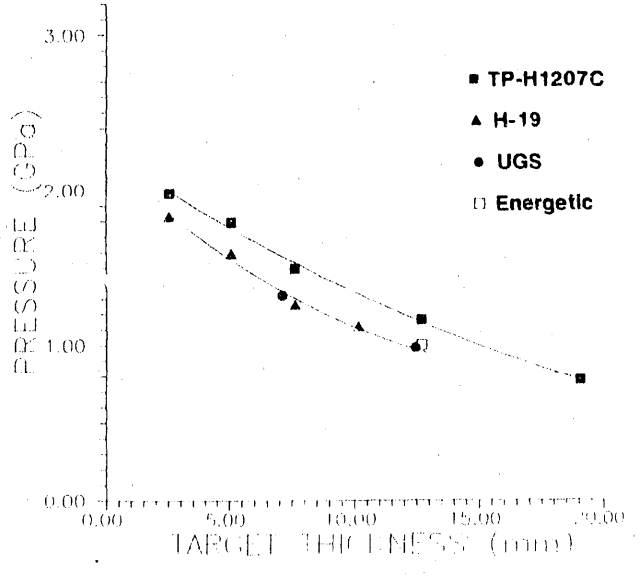

Figure 10. Attenuation profiles for H-19, TP-H1207C, UGS, and the energetic propellant

Discussion

Two other recent investigations have measured the attenuation of a shock wave in H-19. The first experiment was done by SRI[12] during a study of the dynamic spall strength of H-19 under a hydrostatic preload. An H-19 specimen disk was attached to the inside of a 1.27-cm-thick front wall of a cylindrical Lexan (polycarbonate) cup. A Lexan plug was screwed into the cup to form a pressure chamber. Compressed air was used to preload the specimen to an approximately hydrostatic condition. One stress gauge and one particle velocity gauge were positioned at the interface between the specimen and the Lexan wall. Another particle velocity gauge was located at the rear surface of the 0.75-cm-thick H-19 specimen. The data from the particle velocity gauges for a shot with an input pressure of 1.2 GPa on the H-19 specimen are shown in Figure 11. If the Hugoniot parameters for H-19[1] are used to convert the measured particle velocities to pressures at the front (0.25 mm/μs = 1.24 GPa) and back (0.195 mm/μs = 0.94 GPa) surfaces, the attenuation is ~24% for the 0.75-cm-thick H-19 sample. Figure 10 shows the attenuation profile for H-19 measured in this study. Extrapolating the curve to fit a 0.75 cm-length change beginning at a pressure value of 1.24 GPa gives a value of pressure of ~0.85 GPa. This translates to an attenuation of ~31%, which is in experimentally good agreement with the SRI value of ~24%.

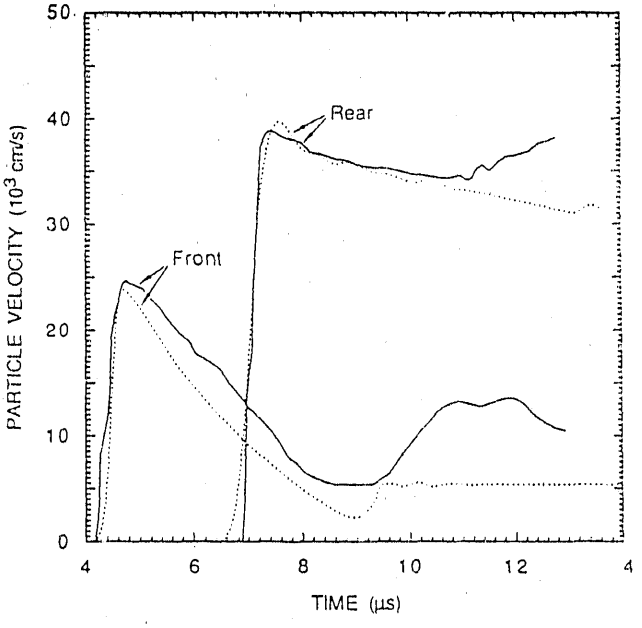

Figure 11. Particle velocity at the front and rear of the H-19 target (SRI)

The second investigation on the attenuation of shock waves in H-19 was done at K-Tech Corp. by Greb.[13] This study also investigated the transmission of longer shock pulses through H-19. The experimental configuration of the PMMA flyer plates/aluminum projectiles was different from the present work in that a quartz gauge was sandwiched between the PMMA flyer plate and aluminum projectile to measure impact stress. A more significant difference was the use

of carbon stress gauges at the rear of the specimens and between PMMA buffer and backer plates at K-Tech instead of the VISAR measurements done at Sandia. The author strongly believes that the use of VISAR measurements for particle velocity and, subsequently, transmitted stress values makes the analysis of the results relatively straightforward and understandable. Examining the K-Tech results, particularly for transmitted wave data, one can see that the gauge produced an additional response depending on the impact pressure. An estimate of the attenuation of the shock pulse by H-19 can be made by subtracting the response of the gauge for a transmission shot at a given impact stress from the response of the gauge for an attenuation shot at a similar impact stress. The results for the K-Tech data using this procedure are given in Table 4. An average value for shock attenuation in H-19 in the stress range of 1.0 to 5.0 GPa is ~20% for a 3-mm-thick specimen. This value agrees reasonably well with an estimated value of 18% from the pressure-sample thickness curve, Figure 4, from the present report for an impact stress of ~2.0 GPa through a 3-mm-thick sample.

Most other studies on propellants and explosives investigated the sensitivity and initiation properties of these materials rather than shock attenuation. However, shock attenuation in these materials can sometimes be extracted from the results. One example of this is given by the following analysis from data reported by R. Setchell on PBX-9404,[14] a plastic-bonded explosive. His report shows a plot of particle velocity versus time showing the shock front evolution at the rear surface of PBX-9404 specimens of various thicknesses which have been impacted by fused silica at 3.2 GPa. From the maximum particle velocity for a given specimen thickness and the Hugoniot relationships for PBX-9404 and fused silica, the pressure can be calculated. These values are plotted as a function of specimen thickness in Figure 12. The attenuation curve determined for TP-H1207C is also shown on this figure for comparison. It appears that shock attenuation is more rapid in PBX-9404 than in TP-H1207C.

Table 4. K-Tech Corp. Transmission Data

Transmission			Attenuation			
			Adjusted			
Impact Stress (GPa)	Gauge Stress (GPa)	Change (%)	Impact Stress (GPa)	Impact Stress (GPa)	Gauge Stress (GPa)	Change (%)
0.199	0.184	07.5	0.189	0.175	0.168	04
0.482	0.430	10.8	0.208	0.192	0.142	24
1.104	0.830	24.8	0.520	0.463	0.289	33
2.059	1.518	26.3	0.995	0.761	0.632	17
3.105	2.359	24.0	3.147	2.392	1.825	24
6.178	4.909	20.5	5.283	4.200	3.503	17

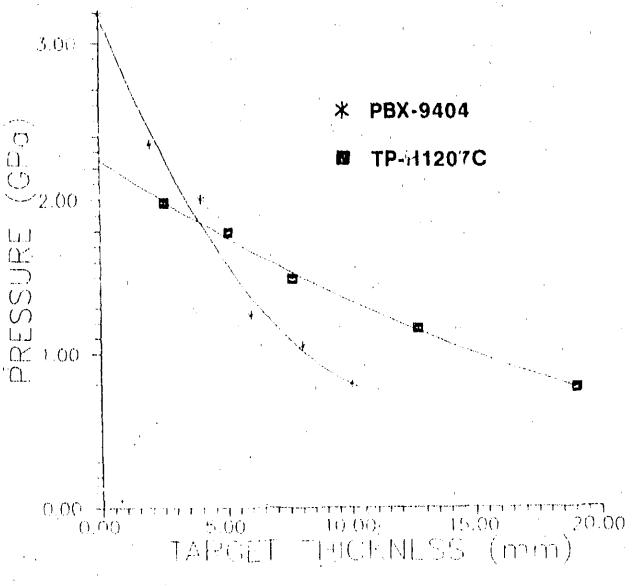

Figure 12. Attenuation profile for PBX-9404 from Setchell

Summary

A series of attenuation experiments on a composite propellant, an energetic propellant, and their simulants was recently completed on a light-gas gun. An initial impulse of 2.0 GPa magnitude and ~0.6 μs duration was imposed upon samples of various thicknesses. VISAR was used to measure the free-surface velocity at the back of the samples, thus giving a curve of attenuated particle velocity versus sample thickness for each material. From the known Hugoniot parameters for each material, the attenuated particle velocities were converted to attenuated shock pressures. A plot of attenuated pressures versus sample thickness is the shock attenuation for that material. Results showed that all four materials attenuated the shock wave very similarly. Material thicknesses of 3.0, 7.62, 12.7, and 19.0 mm attenuated the shock wave ~16%, 33%, 50% and 66%, respectively.

References

[1]L. J. Weirick, "Characterization of Booster-Rocket Propellants and Their Simulants," *1989 Ninth Symposium on Detonation*, Volume I, Paper No. 157, Portland, OR, August 28 – September 1, 1989.

[2]L. R. Green, E. James, and E. Lee, "The Detonability of Composite Propellants," *1986 JANNAF Propulsion Systems Hazards Subcommittee Meeting* Vol. 1, CPIA Pub. 446, March 1986.

[3]L. R. Green, E. James, E. Lee, E. Nidick, and E. Chambers, *Air Force Propellant Study*, UCID 19041, Lawrence Livermore National Laboratory, Livermore, CA, May 1981.

[4]P. Urtiew, E. James, and K. Scribner, *High-Energy Propellant Safety (HEPS) Program. Highlights, Volume I*, UCID 17272-79-3, Lawrence Livermore National Laboratory, Livermore, CA, 1979.

[5]L. Green, E. Chambers, E. James, E. Lee, and A. Weston, *Summary Report on Experimental Work Using the 155-mm Gun*, UCID 19424, Lawrence Livermore National Laboratory, Livermore, CA, June 1982.

[6]C. S. Speight, "Observation of Spallation and Attenuation Effects in Aluminum From Free-Surface Velocity Measurements," Foulness Division Note FDN 4/71 (1971).

[7]M. E. Kipp and R. J. Lawrence, *WONDY V-A One-Dimensional Finite-Difference Wave Propagation Code*, SAND81-0930, Sandia National Laboratories, Albuquerque, NM, June 1982.

[8]W. F. Dunn to L. W. Poulter, "Extended Ambient Cure of H-19 Propellant," Morton-Thiokol Inc., Wasatch Operations, Brigham City, Utah, memo dated 12 October 1987.

[9]S. A. Sheffield and D. W. Dugan, "Description of a New 63-mm Diameter Gas Gun Facility," *Shock Waves in Condensed Matter*, Y. M. Gupta, ed., Plenum Press, 1986.

[10]L. M. Barker and R. E. Hollenbach, "Laser Interferometer for Measuring High Velocities of Any Reflecting Surface," *J. Appl. Phys.* 43:11 (November 1972).

[11]W. F. Hemsing, "Velocity Sensing Interferometer (VISAR) Modification," *Rev. Sci. Instrum.* 50:1 (January 1979).

[12]B. S. Holmes, J. K. Gran, and D. C. Erlich, "Pulsed Laser Target Response (LTH-3)," *Monthly Progress Report* No. 12, SRI International, Menlo Park, CA, March 12, 1989.

[13]A. Greb, *Shock Characterization of Two Simulant Propellants: H-19 and PR-1592*, KTECH/TR-88/32, K-Tech Corp., Albuquerque, NM, November 1989.

[14]R. E. Setchell, "Short-Pulse Shock Initiation of Granular Explosives," *Proceedings of the Seventh Symposium (International) on Detonation*, Naval Surface Weapons Center, White Oak, MD, NSWC MP 82-334, 1982, p. 857.

- END -

DATE FILMED

10 / 22 / 90